Int J Earth Sci (Geol Rundsch) (2017) 106:2575–2592
DOI 10.1007/s00531-017-1447-z

ORIGINAL PAPER

New paleomagnetic results from Upper Cretaceous arc-type rocks from the northern and southern branches of the Neotethys ocean in Anatolia

Mualla Cengiz Cinku[1] · Friedrich Heller[2] · Timur Ustaömer[1]

Received: 8 June 2016 / Accepted: 15 January 2017 / Published online: 20 March 2017

Abstract A paleomagnetic study of Cretaceous arc type rocks in the Central-Eastern Pontides and in the Southeastern Taurides investigates the tectonic and paleolatitudinal evolution of three volcanic belts in Anatolia, namely the Northern and Southern Volcanic Belts in the Pontides and the SE Taurides volcanic belt. The paleomagnetic data indicate that magnetizations were acquired prior to folding at most sampling localities/sites, except for those in the Erzincan area in the Eastern Pontides. The Southern Volcanic Belt was magnetized at a paleolatitude between $23.8^{+4.2}_{-3.8}$°N and $20.2^{+1.3}_{-1.2}$°N. Hisarlı (J Geodyn 52:114–128, 2011) reported a more northerly paleolatitude ($26.6^{+5.1}_{-4.6}$ °N) for the Northern Volcanic Belt. The comparison of the new paleomagnetic results with previous ones in Anatolia allows to conclude that the Southern Volcanic Belt in the Central-Eastern Pontides was emplaced after the Northern Volcanic Belt as a result of slab-roll back of the Northern Neotethys ocean in the Late Cretaceous. In the Southeast Taurides, Upper Cretaceous arc-related sandstones were at a paleolatitude of $16.8^{+4.2}_{-3.8}$. The Late Cretaceous paleomagnetic rotations in the Central Pontides exhibit a counterclockwise rotation of $R \pm \Delta R = -37.1° \pm 5.8°$ (Group 1; Çankırı, Yaylaçayı Formation) while Maastrichtian arc type rocks in the Yozgat area (Group 2) show clockwise rotations $R + \Delta R = 33.7° \pm 8.4°$ and $R + \Delta R = 29.3° \pm 6.0°$. In the SE Taurides counterclockwise and clockwise rotations of $R \pm \Delta R = -48.6° \pm 5.2°$ and $R \pm \Delta R = +34.1° \pm 15.1°$ are obtained (Group 4; Elazığ Magmatic Complex). The Late Cretaceous paleomagnetic rotations in the Pontides follow a general trend in concordance with the shape of the suture zone after the collision between the Pontides and the Kırşehir block. The affect of the westwards excursion of the Anatolian plate and the associated fault bounded block rotations in Miocene are observed in the east of the study area and the SE Taurides.

Key words Paleomagnetic · Upper Cretaceous · Pontides · Taurides · Neotethys Suture Zone

Introduction

The Anatolian plate, which forms part of the southern Eurasian margin, is composed of a series of microcontinents or terranes (Fig. 1) that are separated by suture zones (Şengör and Yılmaz 1981; Robertson and Dixon 1984; Yılmaz et al. 1997a, b). The Pontide (P) terranes rifted off Gondwana in the Ordovician (Okay et al. 2008), whereas the Anatolide–Taurides (A–T) rifted off Gondwana during the Early Mesozoic (Şengör and Yılmaz 1981). The A–T and P microcontinents are separated by branches of the Neotethys ocean (Robertson et al. 2013, 2014). The northern branch of the Neotethys ocean, was closed during the Early Eocene as a result of the collision between the Kırşehir Block and the Pontides (Şengör and Yılmaz 1981; Yılmaz et al. 1997a, b; Rice et al. 2006; Kaymakçı et al. 2009). A large Andean-type volcanic arc formed along the Central to Eastern Pontides as a result of northward subduction below Eurasia, which we refer to as the Northern Volcanic Belt (NVB). The NVB runs parallel to the Black Sea and extends from Samsun to Hopa (Fig. 1). To the south of the

✉ Mualla Cengiz Cinku
mualla@istanbul.edu.tr

[1] Faculty of Engineering, Department of Geophysical Engineering, Istanbul University, 34320 Avcılar/istanbul, Turkey

[2] Department of Earth Sciences, Institute of Geophysics, Sonneggstrasse 5, ETH Zurich, 8092 Zurich, Switzerland

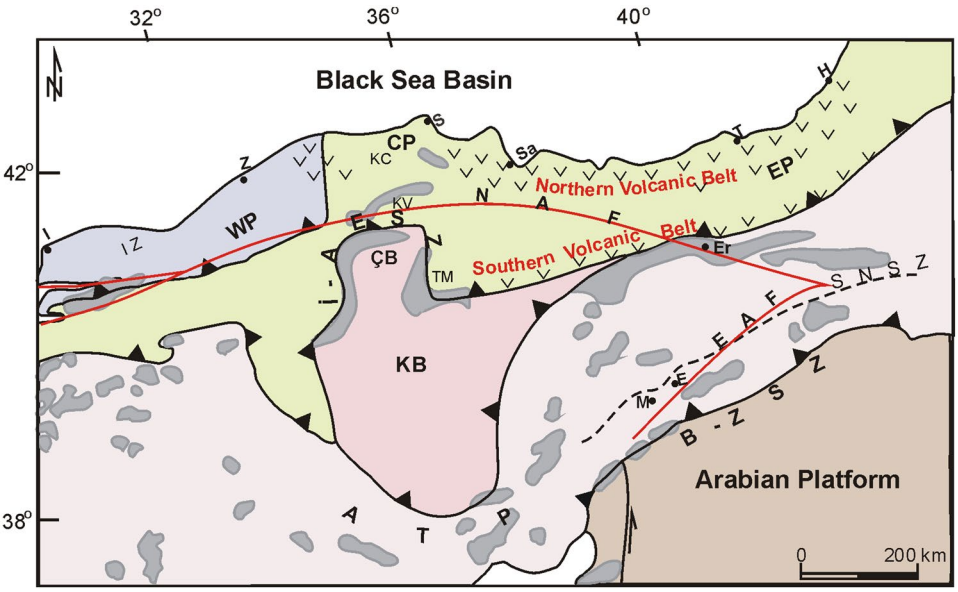

Fig. 1 Main tectonic units of Anatolia and adjacent regions (*gray coloured* patches denote ophiolitic rocks) (modified after Okay and Tüysüz 1999). *ATP* Anatolide Tauride Platform, *CP* Central Pontides, *EP* Eastern Pontides, *IZ* Istanbul Zone, *EAF* East Anatolian Fault, *NAF* North Anatolian Fault, *BZSZ* Bitlis Zağros Suture Zone, *IAESZ* İzmir Ankara Erzincan Suture Zone, *SNSZ* South Neotethys Suture Zone, *ÇB* Çankırı Basin, *KC* Küre Complex, *KV* Kösdağ Volcanics, *TM* Tokat Massif, *E* Elazığ, *Er* Erzincan, *H* Hopa, *İ* İstanbul, *M* Malatya, *Sa* Samsun, *S* Sinop, *T* Trabzon, *Z* Zonguldak

NVB, a second volcanic zone, the E–W trending Southern Volcanic Belt (SVB) traces the North Anatolian Fault (Rice et al. 2006, 2009), and is delimited to its south by the omega-shaped northern tip of the Kırşehir Block. The rocks emplaced in the SVB are ophiolites and overlying arc volcanic rocks that are the easterly extension of the central Pontides (Fig. 1; Yılmaz et al. 1997a, b).

The southern Neotethys, which separated the Arabian Platform in the south from the Anatolide–Tauride Platform in the north, opened in the Late Triassic and closed in the Early Miocene as a result of collision between Arabia and Eurasia (Şengör and Yılmaz 1981; Yılmaz et al. 1997a, b; Robertson et al. 2007a, b; Gans et al. 2009; Okay et al. 2010). Alternative age data were reported as Late Cretaceous (Karig and Kozlu 1990, 1997; Beyarslan and Bingöl 2000); or Late Eocene (Boulton et al. 2006; Boulton 2009). An E–W trending ophiolitic belt was emplaced along the collision front and is known as the Bitlis-Zağros-Suture Zone (Şengör 1984; Yılmaz 1993; Stampfli et al. 2000; Robertson et al. 2007a, b, 2009; Parlak et al. 2009). Plutonic, volcanic, subvolcanic and pyroclastic rocks are exposed in the Elazig Magmatic Complex, which was formed as a result of arc magmatism. Ophiolites were tectonically emplaced beneath the Tauride platform and crosscut by I-type calc-alkaline arc granites (Rızaoğlu et al. 2009) mainly during the Late Cretaceous. The arc-related rocks were generated as a result of regional plate convergence on the top of the supra subduction zone-type crust between 83 and 75 Ma (Karaoğlan et al. 2013).

Based on geologic data from the two volcanic belts in the Pontides, we cannot distinguish whether the NVB and SVB resulted from subduction of the same oceanic crust. The paleolatitudinal position of the NVB and SVB during their emplacement, may enable us to knowledge of assess whether the arcs formed above the same subduction zone. Previous paleomagnetic studies from the NVB indicate a paleolatitude of ~26°N (Channell et al. 1996; Meijers et al. 2010; Hisarlı 2011) during the Late Cretaceous. Limited paleomagnetic results from Maastrichtian volcanic and volcanoclastic rocks from the SVB suggest that the SVB was situated farther south, with a paleolatitude of 20.0°N ± 2.5°, of the NVB (Çinku et al. 2010), providing support for a model in which two different subduction zones were responsible for the formation of the NVB and SVB. The absence of paleomagnetic data from Upper Cretaceous arc-type rocks from the southeastern Taurides prevents us to determine the paleolatitude position of the volcanic belt in the South Taurides.

When considering previous paleomagnetic declinations in the Pontides a general trend in counterclockwise sense could be detected in the Central Pontides during the Late Cretaceous. The evidence of an oroclinal bending has been proposed from the earlier study of Meijers et al. (2010) in the Central Pontides. The authors showed evidence of counterclockwise rotation in the western part of the Central Pontides, while only four reliable sites was the evidence of clockwise rotation in the eastern part of the Central Pontides. Instead, Çinku et al. (2011, 2015) reported on the oroclinal bending on the İZEZS between the collision of the Pontides and the Niğde-Kırşehir Massif during the Late Cretaceous and Middle Eocene. In the study of Cengiz Çinku et al. (2016) the different senses of rotations in the central, SE Taurides, and the Niğde-Kırşehir Massif during the Late Cretaceous-Middle Eocene are interpreted as two-phase oroclinal bending

after the emplacement of the ophiolitic slices, first in the SE Taurides and later in the central Taurides.

To contribute to a solution of the Anatolian paleogeographic puzzle, a total of 42 paleomagnetic sites were established in Upper Cretaceous arc type volcanic rocks and their associated sedimentary rocks in the Central-Eastern Pontides and the Southeastern Taurides. The new data provide insight on the approximate position of the subduction zones active in the Anatolian Tethyan realm during the Late Mesozoic.

Regional geology

The study area includes major continental fragments of the Central and Eastern Pontides.(Fig. 1). The İzmir-Ankara-Erzincan Suture Zone (İAESZ; northern Neotethys) extends along these fragments in an E–W direction. Farther south, the study area comprises the Taurides, which are limited to south by the southern Neotethys Suture Zone and the Inner-Tauride Suture Zone to the N (Fig. 1).

The Central Pontides are situated between the Kırşehir Block to the south and the Black Sea to the north (Fig. 1). The basement rocks consist of the Permo-Carboniferous granitoids (Okay et al. 2015) and Triassic-Early Jurassic Küre Complex (Ustaömer and Robertson 1993, 1994). The Küre Complex was intruded by Mid-Jurassic granitoids and deformed by thrusting and folding in the Late Jurassic. An Upper Jurassic-Lower Cretaceous sedimentary succession lies unconformably on the deformed Küre Complex, similar to the İstanbul Zone in northwest Turkey. An Aptian-Albian flyschoidal sequence with olistoliths of Upper Jurassic-Lower Cretaceous limestone blocks overlies Middle Jurassic shallow level intrusions and records crustal extension and basin formation (Tekeli 1981; Tüysüz 1990; Görür and Tüysüz 1997; Ustaömer and Robertson 1997). This flysch succession is interpreted to comprise syn-rift sediments related to the opening of Western Black Sea Basin. The Late Cretaceous to Lower Cenozoic succession lies unconformably on the Lower Cretaceous syn-rift sedimentary rocks and is represented by pink pelagic limestones, marls and volcanic rocks (Görür and Tüysüz 1997; Tüysüz 1999; Tüysüz et al. 2012). South of the Küre complex, $^{40}Ar/^{39}Ar$ dating on phengites yields an age of about 112–106 Ma for the metamorphism of Lower Creatceous turbidites (Okay et al. 2013), while farther south, ages of 90 Ma were obtained from the Kösdağ volcanic rocks (Aygül et al. 2015).

The Eastern Pontides are represented by a metamorphic complex that belongs to the Hercynian basement of the Eastern Pontides orogenic belt, e.g. the Pulur massif (Yılmaz et al. 1993, 1997a, b) in the southernmost part (Fig. 1). The Late Cretaceous Eastern Pontides magmatic arc rocks in the NVB constitute magmatic and granitic rocks and change laterally southward into volcanogenic flysch sequences [e.g., the Beldağ group (Yılmaz et al. 1997a, b)]. Farther South in the SVB, ultramafic rocks and Late Cretaceous ophiolitic rocks are widespread.

The ophiolitic rocks transected by the North Anatolian Fault (Fig. 1) are squeezed between the Pontides and the Kırşehir Block and are interpreted to be a part of the İzmir-Ankara-Erzincan Suture Zone. On the Kırşehir Block, MORB and supra-subduction zone ophiolitic fragments are intruded by granites (Floyd et al. 1998; Boztuğ 2000; Yalınız et al. 2000; Robertson and Dixon 1984; Göncüoğlu et al. 1991; İlbeyli et al. 2004; Kadıoğlu et al. 2006; Robertson et al. 2009). Radiometric data based on $^{207}Pb–^{206}Pb$ zircon evaporation ages show that the granites were emplaced between 94.6 ± 3.4 and 74.9 ± 3.8 Ma (Boztuğ et al. 2007). During the collision between the Pontides and the Kırşehir Block in the Latest Cretaceous (Nairn 2011; Nairn et al. 2012; Lefebvre et al. 2013) or Early Eocene (Yılmaz et al. 1997a, b) ophiolitic rocks were emplaced along the Çankırı basin. The Çankırı Basin in the northern part of the Kırşehir Block separates the Pontides and the Kırşehir continental fragments from each other. The basin is surrounded by the North Anatolian Ophiolitic Belt. Thrusts and faults which developed during collision between the Kırşehir Block and the Pontides define the western and northern rims of the Çankırı basin (Kaymakçı et al. 2003). In the South of the Çankırı basin, ophiolitic rocks are thrust over Late Cretaceous-Early Cenozoic granitic rocks (İlbeyli et al. 2004; Boztuğ and Jonckheere 2007) or are defined as epi-ophiolitic cover and related arc-type rocks (Yalınız et al. 2000).

In the northern part of the Kırşehir Block, Campanian–Maastrichtian arc volcanic rocks and volcaniclastic sandstones of the Yaylaçayı Formation are exposed (Yoldaş 1982). A Late Cretaceous cover sequence defined by sedimentary rocks of the Yapraklı Formation with a thickness of 500 m rests unconformably on the arc type rock sequences (Birgili et al. 1974). The North Anatolian Ophiolite Belt continues farther east along the Eastern Pontides, where it consists mostly of ophiolitic rocks and arc volcanic rocks. These Upper Cretacaeous rocks are thrust southwards onto Mesozoic sedimentary rocks (Rice et al. 2006). Farther North, the NVB that formed on the Late Cretaceous continental margin above a northward-subducting oceanic lithosphere is exposed (e.g. Şengör and Yılmaz 1981; Yılmaz et al. 1997a, b; Okay and Şahintürk 1997). This belt, which is described as the NVB, is the eastern extension of the volcanic arc in the Central Pontides. The Tokat massif in the south of the Eastern Pontides is composed of range of metamorphic and ophiolitic rocks (Yılmaz et al. 1997a, b). The ophiolitic rocks belong to the İAESZ and are named

of Yeşilırmak Group (Özcan et al. 1980; Yılmaz et al. 1997a, b).

The southern margin of Southeast Anatolia is represented by part of the regional Tauride Platform (Şengör and Yılmaz 1981; Özgül and Turşucu 1984). Although the basement of the Western Pontides (İstanbul Zone) is Eurasia-derived (Şengör 1979; Okay et al. 1996; Yiğitbaş et al. 1999; Bozkurt et al. 2008), the basement rocks of the Tauride Platform have similar stratigraphy and age as the Gondwanan Arabian plate (Şengör and Yılmaz 1981; Kröner and Şengör 1990; Yılmaz 1993; Robertson et al. 2009). The Tauride Platform consists of a stack of thrust sheets, containing Palaeozoic to lower Cenozoic carbonate platform successions and associated sedimentary rocks. Ophiolitic rocks and associated arc type rocks derived from the Southern Neotethys ocean were emplaced on top of the Tauride platform (Robertson et al. 2007a, b; Parlak et al. 2009; Rızaoğlu et al. 2009; Karaoğlan et al. 2013). The arc-type rocks are unconformably overlain by volcanic and sedimentary rocks of the Eocene Maden complex (Perinçek 1979; Aktaş and Robertson 1984; Yiğitbaş and Yılmaz 1996; Robertson et al. 2006), which is widely distributed in the Southeast Taurides. The volcanic–sedimentary lithologies are dated as Late Campanian–Early Maastrichtian, based on planktic Foraminifera assemblages (Michard et al. 1984; Yazgan and Chessex 1991).

Paleomagnetic sampling and techniques

Paleomagnetic sampling

In this study, 42 sites distributed in four areas were sampled. Three of the selected areas (Groups 1–3) are located along the IAESZ in arc type volcanic and volcanoclastic sandstones, and one selected area is located in the southern Taurides arc lavas and volcanoclastic deposits (Group 4; Figs. 2, 3). Sampling sites were collected from (1) north of Çankırı on the Campanian–Maastrichtian Yaylaçayı Formation (Yoldaş 1982) (six sites, PT 15–20), (2) Maastrichtian rocks NE of Yozgat (Erdoğan et al. 1996) (seven sites, PT26-32), and (3) from the Campanian–Maastrichtian Karadağ Formation (Rice et al. 2006) in Erzincan (ten sites, PT36-45). Finally, in the southeast Taurides, Campanian–Maastrichtian arc lavas and volcanic sandstones were sampled at 19 sites from the Elazığ magmatic complex

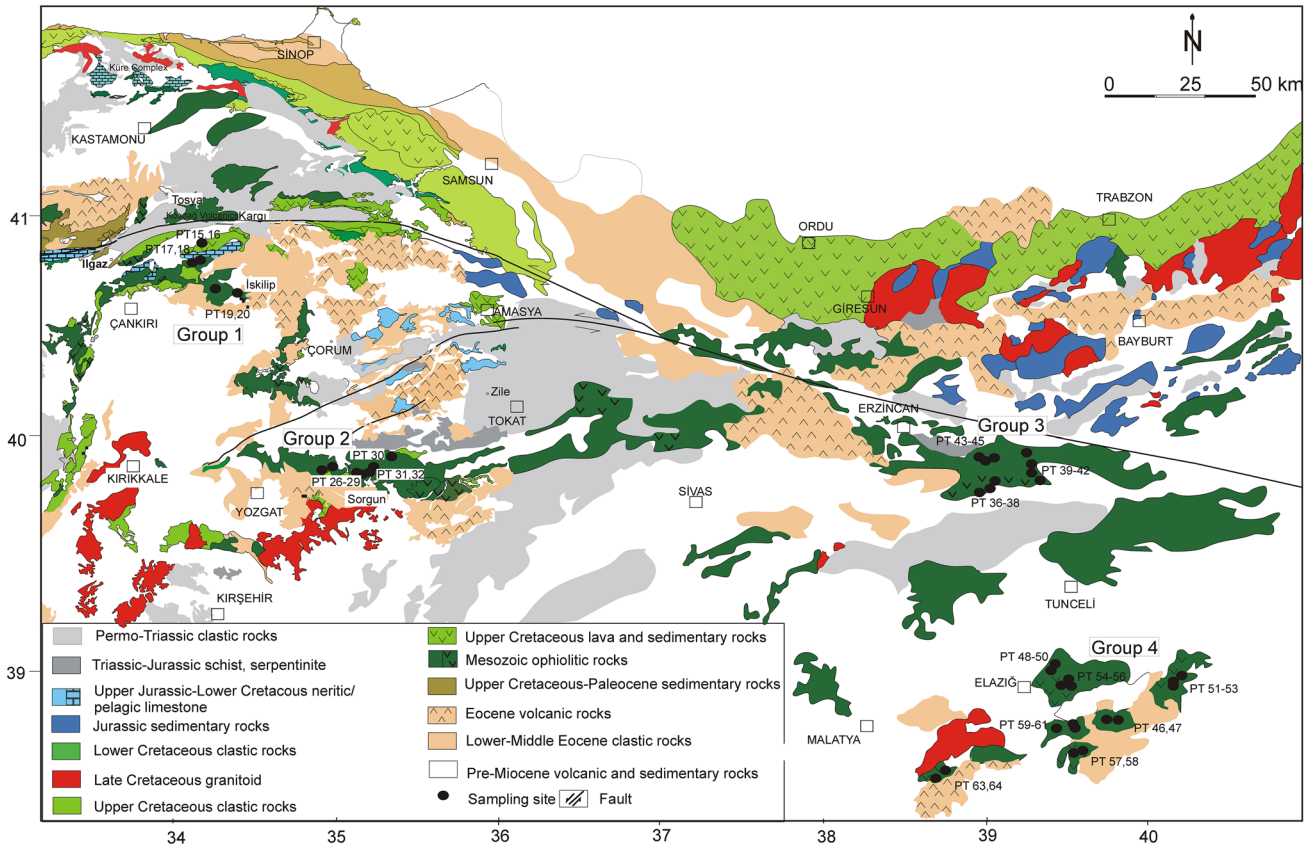

Fig. 2 Geologic map with numbered sampling site locations for the Pontides and Southeast Taurides (geologic map modified from the 1:500000 MTA 2002 geologic map). *A* Çankırı Basin, *B* Yozgat, *C* Tokat, *D* Erzincan, *E* Malatya and Elazığ

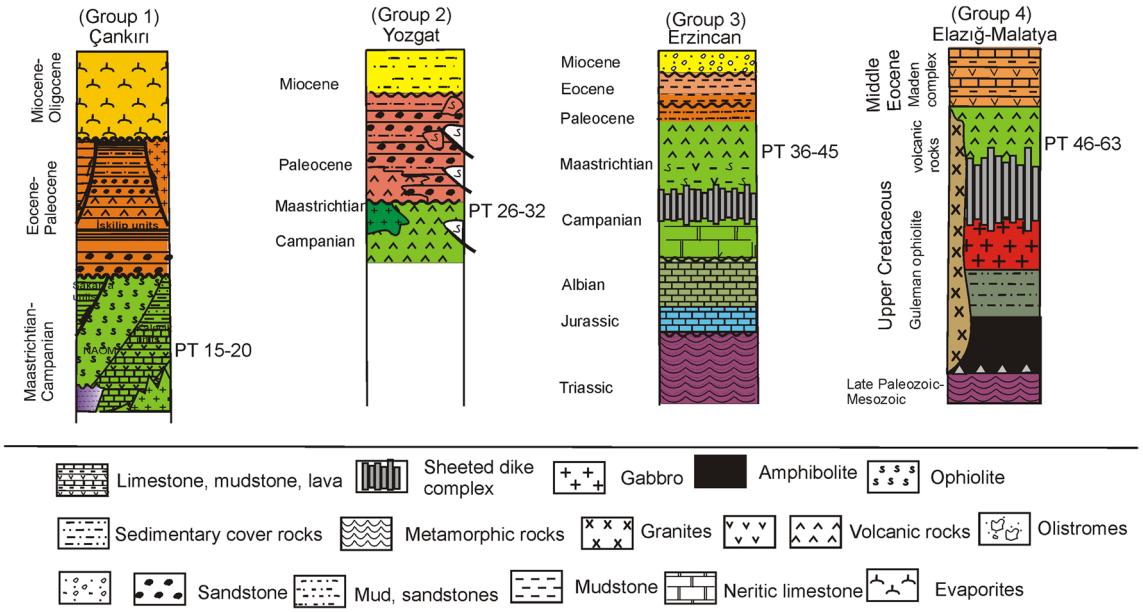

Fig. 3 Generalized stratigraphic columnar sections showing the sampling sites in **a** Çankırı (Kaymakçı et al. 2009; Tüysüz et al. 1995), **b** Yozgat (Erdoğan et al. 1996), **c** Tokat (Yılmaz et al. 1997a, b), **d** Erzincan (Rice et al. 2009) and **e** Elazığ-Malatya (Parlak et al. 2009)

(Perinçek 1979; Yılmaz 1993; Yılmaz et al. 1993; Parlak et al. 2009; Robertson et al. 2007a, b) in the area between Elazığ and Malatya (PT46-64).

Paleomagnetic techniques

A total of 427 samples were cut into standard 2.2-cm long cylindrical specimens and between 7 and 25 paleomagnetic specimens from each site were subjected to both stepwise thermal and alternating field (AF) demagnetization. A motorized portable core drill was used to collect core samples. Sample orientation was determined using both magnetic and sun compasses. The differences between the magnetic and sun compass readings of about 5°.

The rock magnetic analyses performed to determine the ferromagnetic minerals as a result of hysteresis curves, thermomagnetic curves, isothermal remanent magnetization curves and three-axis IRM curves. The hysteresis curves were preformed on 0.5 cm^3 powdered samples representative for each site were measured in fields up to 1 T using a Princeton Measurements Corporation MicroMag magnetometer (Model 3900) at the Tübingen University paleomagnetic laboratory. Thermomagnetic curves, measuring the temperature dependence of the magnetic susceptibility were done in 50 selected samples between 0.465 and 4.6 kHz, heating 3 g of powder sample in air between room temperature and 700 °C using a MS2 Bartington susceptibility meter at the University of Istanbul Yılmaz İspir paleomagnetic laboratory. Isothermal remanent magnetization (IRM) acquisition curves were obtained for one specimen per site up to maximum fields of 1 T along the cylindrical sample *Z*-axis with an ASC pulse magnetizer. The Lowrie (1990) test (i.e. thermal demagnetization of a three-axis IRM, Lowrie 1990) was performed by applying fields of 1 T along the *Z*-axis (hard component), 0.4 T (medium component) along the Y-axis and 0.12 T (soft component) along the sample *X*-axis. Subsequently, samples were thermally demagnetized to identify the magnetic carriers based on their coercivity and thermal unblocking behaviour.

The directions and intensities of the natural remanent magnetization (NRM) were measured with a 2G Enterprises 755R three-axes DC-SQUID cryogenic magnetometer at the University of Tübingen, Germany and a JR-6 spinner magnetometer (AGICO) in the Yılmaz Ispir Paleomagnetism Laboratory of Istanbul University, Turkey. Both thermal and alternating field demagnetization were applied to isolate the characteristic remanent magnetizations (ChRM) of steps between 50 and 700 °C or 2.5–150 mT, respectively, using a Schonstedt MTD-80/ Magnetic Measurements MTD 80 oven and a 2G600 AF/LDA5 AF demagnetizer. Magnetization components were identified and directions calculated using orthogonal vector projections (Zijderveld 1967). Principal component analysis (Kirschvink 1980) was used to calculate the directions of individual NRM components. Fisher's (1953) methods were used to calculate site mean directions and associated statistics. Paleomagnetic fold test was applied using the methods of McFadden (1990) and McElhinny (1964)and Enkin and Watson (1996).

To determine the angular standard deviation of the virtual geomagnetic poles for each site, we used the criteria developed by Deenen et al. (2011). This criteria is statistically expressed by A95 confidence limits (A95max and A95min), and the number of samples (*N*) per site.

Results

Rock magnetism

Thermomagnetic analysis shows mostly similar behaviour among samples of volcanic and those of sedimentary rocks (Fig. 4). The main magnetic phase for most sites is titanomagnetite (Fig. 4a1, b1), although there are some samples

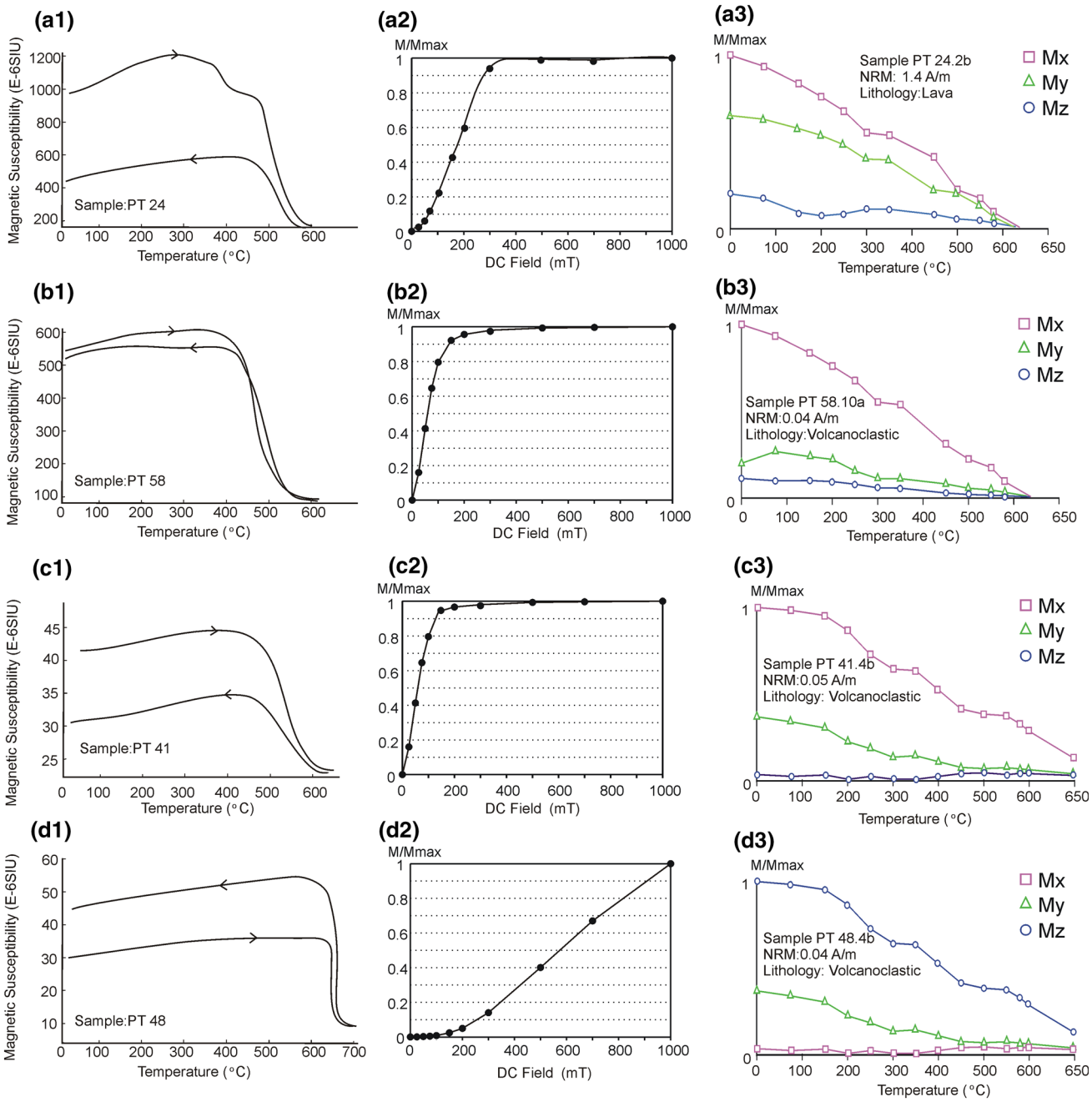

Fig. 4 Thermomagnetic (X vs T) *curves* of representative samples showing the presenceof titanomagnetite (**a1, c1**) and titanohematite (**d1**). Normalized remanent magnetization IRM acquisition curves (**a2–d2**) and thermal demagnetization results of three-axial IRM (**a3–d3**): hard M_z, medium M_y, and soft M_x axis (relative to the applied magnetic field and hence, the coercivity of the magnetic mineral)

showing Curie temperature which exceed 580 °C, indicating further oxidation of the maghemite-hematite phases (Fig. 4c1). Some heating curves of the volcanic rocks show a small drop around 400 °C that is representative for Ti-rich titanomagnetite or the transformation to maghemite (Fig. 4a1). In most sedimentary and volcanic samples, the differences between heating and cooling curves indicate a significant degree of alteration (Fig. 4a1, c1), while for the remaining 30% of the samples a reversible behaviour is observed (Fig. 4b1). In some sandstone samples, the main magnetic phase is identified as hematite (Fig. 4d1). The susceptibility increase upon cooling can be explained by the growth of new maghemite in the presence of reduced oxygen partial pressure in the heating chamber at high temperature (Fig. 4d1). A decrease in susceptibility upon cooling (Fig. 4a1, c1) is due to decomposition and oxidation of titanomagnetite to maghemite or hematite (Dunlop and Özdemir 1997).

IRM acquisition curves show two different types of behavior as observed with the thermomagnetic curves. The first type is dominated by low to moderate coercivity phases with saturation reached by 0.1–0.3 T (Fig. 4a2, b2, c3). Taking the thermomagnetic evidence into account, the low-coercivity mineral is likely to be titanomagnetite in variable oxidation state as can be seen in the three-axis thermal demagnetization plots (Fig. 4a3, b3, c3). Another type of IRM is characterized by a minimum increase of magnetization in low fields (up to 1 T), often without complete saturation at 1 T (Fig. 4d2). This high-coercivity phase likely represents (titano-) hematite as it is evident from the the Néel temperature in Fig. 4d1 and the three-axis demagnetization plot (Fig. 4d2). In this case, the intermediate coercivity phase as the second strongest component of the IRM, may be associated with maghemite.

Magnetic grain sizes were estimated by plotting hysteresis properties on a Day plot (Day et al. 1977; Dunlop 2002; Fig. 5). A saturation remanence versus saturation magnetization ratios (Jrs/Js) of about 0.1–0.5, and a coercivity of remanence versus coercivity ratios (Hcr/Hc) of about 1.7–3.4 place general ensemble of the (titano)magnetite grains into the pseudo-single-domain (PSD) grain size. A number of samples fall into the superparamagnetic grain size, which do not show any paleomagnetic remanence.

Paleomagnetic analysis

The NRM intensity ranges between ~30mAm^{-1} for the volcanoclastic rocks and between 100 and 4560 mAm^{-1} for the volcanic rocks. Most specimens have a viscous component with a random direction that is demagnetized below 0–25 mT or 0–250 °C (Fig. 6 b, o, r and a, c, d–f, h, j, k, m). The ChRM direction is largely isolated between 450 and 580 °C in most samples (n, o, p, r, s), but high laboratory

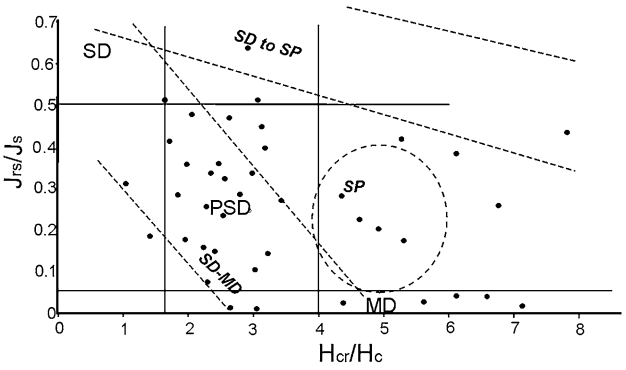

Fig. 5 Hysteresis parameters on the Day plot (Day et al. 1977). *SD* single domain, *PSD* pseudosingle domain, *MD* multidomain, *SP* superparamagnetic dominated regions. *Dashed lines* refer to the titano (magnetite) grain size fields as defined by Dunlop (2002)

unblocking temperatures above 600 °C indicate the presence of a high temperature component in some samples (Fig. 6b, l). For all the samples that show well-defined consistent behaviour during demagnetization, a maximum angular deviation (MAD) < 5° was obtained for the characteristic remanent magnetization (ChRM).

From a total of 42 sites, 12 sites were rejected due to (a) a limited number of specimens ($N < 6$) or because the estimated site mean with large uncertainties ($\alpha_{95} > 15$º; sites PT 18, 30, 35, 39, 61), (b) unstable behaviour during demagnetization PT 46, 47, 55, 64 or (c) due to insufficient isolation of the ChRM component (PT 50) (d) sites with a mean ChRM direction that is very different from those of other sites from a certain group (PT 43, 44).

Paleomagnetic mean directions

Group 1: Çankırı (Yaylaçayı Formation)

Arc type volcaniclastic rocks from the northern segment of the İAESZ in the Central Pontides (NVB) ($N = 5$ sites) yield $D = 312.7°$, $I = 21.0°$, $\alpha_{95} = 33.7°$ in in situ coordinates, and $D = 311.6°$, $I = 39.5°$, $\alpha_{95} = 6.6°$ after tilt correction from three reverse and two normal polarity sites (Table 1; Fig. 7a). The precision parameter increases to a value of ks/kg: 22.2 and critical values at 95%:6.39 and 99%:16.0, at the 99% confidence level in the McElhinny (1964) fold test. When applying the progressive fold test of McFadden (1990) a maximum k value is obtained at 102% unfolding. The k-ratio and fold test results are interpreted to indicate that the magnetization was acquired prior to folding.

Group 2: Yozgat

In the Yozgat area, we grouped the volcanic and volcaniclastic sandstones separately. For the sedimentary rocks

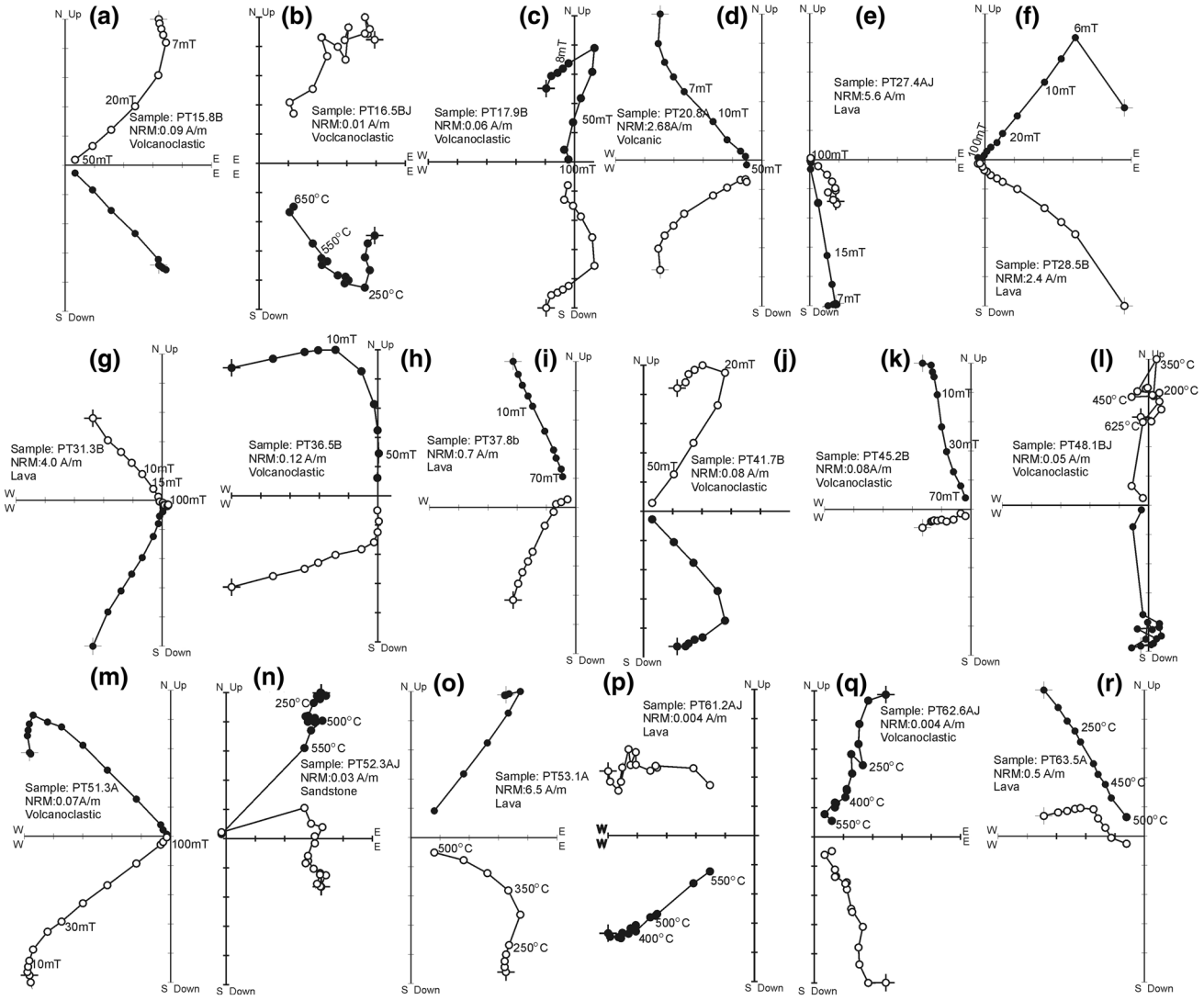

Fig. 6 Zijderveld (1967) orthogonal demagnetization diagrams shown in stratigraphic coordinates, of representative samples during stepwise thermal and alternating field demagnetization (in degrees Celsius and mT). *Solid* (*open*) symbols for horizontal (*vertical*) components, respectively

(Group 2(S)), group mean directions ($N=3$) of $D=79.4°$, $I=12.6°$, $\alpha_{95}=97.9°$ and $D=18.0°$, $I=35.6°$, $\alpha_{95}=18.2°$ are obtained before and after tilt correction, respectively (Table 1; Fig. 7b). The precision parameter increases to a value of kg/ks: 17.3 with the critical values of 6.39 at the 95% confidence level and 16.0 at the 99% confidence level in the McElhinny (1964) fold test. In the McFadden (1990) fold test the precision parameter reaches a maximum at 116% unfolding. The volcanic rocks [Group 2 (L)] show a group mean direction ($N=3$ sites) with $D=19.6°$, $I=40.0°$, $\alpha_{95}=67.9°$ in in situ coordinates, and $D=19.1°$, $I=36.4°$ and $\alpha_{95}=11.4°$ after tilt correction (Table 1; Fig. 7c). The *k*-ratio reaches the significant value ks/kg: 26.9 (critical values at 95%:6.39 and 99%:16.0). Using the fold test of McFadden (1990), the maximum precision parameter is obtained at 86% unfolding.

Group 3: Erzincan (Karadağ formation)

Seven normal polarity sites from volcanic rocks and volcanoclastic sandstones of the Karadağ arc volcanic sequence in Erzincan show a mean direction (Group 3) in geographic coodinates of $D=347.4°$, $I=53.9°$, $\alpha_{95}=4.7°$ and in the stratigraphic coordinates $D=341.3°$, $I=24.8°$, $\alpha_{95}=14.0°$ (Table 1; Fig. 7d). The palaeomagnetic fold test of Mc Fadden (1990) indicates that the best grouping occurs at 13% untilting. The magnetization, therefore, likely is of post-folding origin.

Table 1 Lower Cretaceous and Late Cretaceous paleomagnetic results from the Pontides and Taurides

Site	Lithology	Lat. (°N)	Long. (°E)	Strike/dip	N/n	Dg	Ig	Ds	Is	α_{95}	k	A95(vgp)	A95 min.	A95 max.
Group 1														
PT15	VS	40.58.564	34.05.551	15/53	8/7	307.0	−6.8	134.8	−41.6	7.7	36.3	12.2	5.2	22.1
PT16	VS	40.57.580	34.05.145	340/42	19/17	106.7	−19.9	129.3	−49.3	7.1	37.2	5.8	3.9	13.8
PT17	VS	40.53.880	34.09.023	40/27	25/18	128.3	−13.5	127.9	−40.5	8.0	29.5	6.7	3.8	13.3
PT18*	VS	40.53.880	34.09.023	40/27	9/6	301.4	−17.2	298.6	43.8	25.9	11.2	–	–	–
PT19	VS	40.54.737	34.09.548	40/8	18/18	321.3	27.0	322.3	34.8	9.7	13.6	7.3	3.8	13.3
PT20	V	40.44.829	34.26.158	175/48	12/12	7.6	54.7	312.2	39.8	11.8	24.4	10.4	4.4	17.1
Mean PT 15, 16, 17, 19, 20 calculate means for $N = 5$						**313.0**	**23.3**			**32.9**	**6.4**			
								313.6	**41.3**	**6.4**	**142.9**			
PT21a	VS	40.18.450	33.36.833	80/18	19/16	38.8	77.3	356.8	11.9	7.3	22.3	**8.2**	4.0	14.3
PT22a	V	40.25.910	34.37.307	205/21	17/17	156.5	28.8	167.8	43.2	4.2	33.7	**11.4**	3.9	13.8
PT23a	VS	40.25.910	34.37.307	205/21	6/6	125.8	35.3	130.8	55.8	4.3	53.2	8.2	5.9	26.5
PT24a	V	40.00.393	34.32.162	85/69	8/8	4.8	48.4	161.4	61.5	7.8	45.4	14.3	5.2	22.1
PT25a	VS	40.00.393	34.32.162	85/69	6/6	59.1	28.7	106.5	32.0	8.5	45.5	8.2	5.9	26.5
Group 2														
PT26	VS	39.54.791	34.56.277	230/23	15/12	51.9	40.7	31.7	36.7	6.3	32.1	6.4	4.4	17.1
PT27	V	39.54.944	35.00.394	230/23	9/8	44.2	48.1	20.1	37.5	4.8	74.0	3.8	5.2	22.1
PT28	V	39.53.700	35.10.299	260/36	12/9	38.2	68.3	11.2	38.3	5.7	80.5	5.6	5.0	20.5
PT29	VS	39.54.750	35.10.299	235/80	15/12	269.3	−32.0	203.5	−34.0	14.1	17.8	13.2	4.4	17.1
PT30*	VS	40.02.191	35.23.709	345/38	8/3	215.2	−25.4	219.5	5.1	27.3	8.4	–	–	–
PT31	V	40.14.567	36.35.435	35/84	14/10	358.1	−0.8	28.1	36.5	5.3	51.3	5.4	4.8	19.2
PT32	VS	40.14.474	36.34.620	315/80	8/8	84.7	−43.4	186.0	−37.0	10.2	30.6	10.3	5.2	22.1
PT33	PL	40.14.315	36.34.234	345/28	9/8	355.0	45.3	17.3	34.2	5.1	62.3	5.3	5.2	22.1
PT34	VS	40.12.872	36.38.290	15/22	16/14	14.7	41.2	33.2	37.5	8.5	42.3	8.6	4.2	15.6
PT35*	VS	40.00.900	36.59.104	335/48	10/7	11.2	49.4	32.4	12.9	24.2	14.4	–	–	–
Mean sedimentary rocks PT 26, 29, 32, 34 calculate means for $N = 4$						**40.4**	**61.4**			**68.6**	**2.8**			
								24.3	**36.6**	**11.1**	**69.8**			
Mean Lavas PT 27, 28, 31, 33 calculate means for $N = 4$						**55.8**	**68.6**			**88.7**	**2.1**			
								19.4	**35.7**	**6.7**	**190.1**			
Group 3														
PT36	VS	39.40.979	39.00.939	225/35	10/10	350.8	64.5	332.4	32.7	5.6	64.2	5.8	4.8	19.2
PT37	V	39.41.123	38.57.520	225/35	20/18	353.7	61.8	333.6	30.0	4.3	71.6	4.4	3.8	13.3
PT38	VS	39.41.421	38.57.826	175/35	14/11	357.2	49.1	322.8	39.3	4.8	93.0	5.1	4.6	18.1
PT39*	VS	39.47.044	39.15.732	225/35	16/4	311.1	55.2	312.6	20.2	28.1	10.4	–	–	–
PT40	VS	39.43.101	39.21.348	237/33	12/10	347.7	56.9	339.3	25.1	10.1	25.3	10.0	4.8	19.2
PT41	VS	39.47.044	39.15.732	307/54	14/10	342.9	47.8	3.8	6.7	7.2	12.5	5.8	4.8	19.2
PT42	VS	39.42.814	39.21.192	310/36	10/7	338.4	51.5	1.9	27.3	8.4	25.2	5.3	5.5	24.1

Table 1 (continued)

Site	Lithology	Lat. (°N)	Long. (°E)	Strike/dip	N/n	Dg	Ig	Ds	Is	α_{95}	k	A95(vgp)	A95 min.	A95 max.
PT43*	VS	39.41.874	39.02.242	215/47	15/10	204.4	82.5	294.7	43.9	9.3	22.1	9.5	4.8	19.2
PT44*	VS	39.43.276	38.59.125	245/47	14/12	260.8	63.3	304.6	31.3	11.1	34.1	10.1	4.4	17.1
PT45	VS	39.43.276	38.59.125	215/47	15/10	342.4	54.2	326.3	12.3	6.9	43.2	6.9	4.8	19.2
Mean PT36, 37, 38, 39, 40, 41, 45 calculate means for $N = 7$						**347.4**	**53.9**			**4.7**	**167.4**			
								341.3	**24.8**	**14.0**	**19.6**			
Group 4														
PT46*	V	38.34.115	39.29.310	116/42	–	–	–	–	–	–	–	–	–	–
PT47*	VS	38.34.533	39.29.386	116/42	–	–	–	–	–	–	–	–	–	–
PT48	VS	38.46.844	39.20.112	345/27	15/15	118.4	−12.8	126.6	−31.3	5.5	49.2	6.0	4.1	14.9
PT49	VS	38.44.320	39.19.147	305/27	8/6	81.6	40.1	71.2	19.6	12.2	40.1	11.2	5.9	26.5
PT50*	VS	38.44.183	39.18.594	305/27	9/9	–	–	–	–	–	–	–	–	–
PT51	VS	38.45.937	39.40.285	160/22	12/10	326.4	39.8	311.4	31.7	5.8	34.3	6.2	4.8	19.2
PT52	V	38.45.931	39.40.224	107/26	9/8	30.1	−2.9	31.1	23.1	6.6	83.6	6.4	5.5	24.1
PT53	V	38.45.931	39.40.224	107/26	9/8	22.5	11.1	23.5	35.5	5.6	85.2	5.2	5.0	20.5
PT54	V	38.41.473	39.23.967	193/36	7/7	23.1	33.6	358.8	32.2	7.8	74.3	7.8	5.5	24.1
PT55*	VS	38.41.473	39.23.967	193/36	–	–	–	–	–	–	–	–	–	–
PT56	V	38.41.343	39.23.664	235/30	10/8	62.0	38.2	42.7	33.1	6.7	68.7	8.0	5.0	20.5
PT57	VS	38.27.798	39.23.773	127/25	14/10	299.2	41.5	280.4	33.9	8.6	32.7	9.5	4.8	19.2
PT58	VS	38.28.210	39.24.768	307/25	8/6	109.0	−27.1	123.2	−32.0	8.6	6.1	8.5	5.9	26.5
PT59	VS	38.31.945	39.29.950	154/35	7/7	142.3	−40.5	120.2	−26.3	13.0	22.4	11.1	5.5	24.1
PT60	VS	38.32.134	39.27.975	188/12	15/10	301.1	44.0	297.7	32.8	11.1	17.3	12.6	4.8	19.2
PT61*	VS	38.32.164	39.27.995	188/12	9/7	126.1	−29.1	123.7	−18.4	25.2	11.4	–	–	–
PT62	VS	38.31.792	39.25.146	188/12	14/12	125.3	−43.5	121.2	−32.6	8.9	27.3	8.4	4.4	17.1
PT63	V	38.22.608	38.40.110	195/86	10/8	58.6	50.4	317.3	29.9	7.5	66.3	8.2	5.5	24.1
PT64*	VS	38.21.782	38.39.558	137/21	8/8	–	–	–	–	–	–	–	–	–
Mean sedimentary rocks PT48, 49, 51, 57, 58, 59, 60, 62, 63 Calculate means for $N = 7$						**131.1**	**−43.0**			**22.3**	**7.1**			
								121.5	**−32.7**	**6.4**	**77.0**			
Mean Lavas PT52, 53, 54, 56 Calculate means for $N = 4$						**38.2**	**50.3**			**129.9**	**1.5**			
								24.5	**32.3**	**19.2**	**23.9**			

Site numbers, lithology, geographic location [Lat. (°N) Long. (°E)] and bedding attitudes are given first. *N* denotes number of samples per locality, *n* the number of samples used for site mean calculation. Declination $D_{g(s)}$ and inclination $I_{g(s)}$ describe the mean directions in geographic (before tilt correction) and stratigraphic coordinates (after tilt correction), respectively. α_{95} is the 95% confidence circle, *k* is the precision parameter (Fisher 1953). Sites with asterisk (*) were not considered for tectonic interpretation for reasons given in the text. Sites with index a ([a]) are reported in the study of Çinku et al. (2014)

The bold define the group mean direction

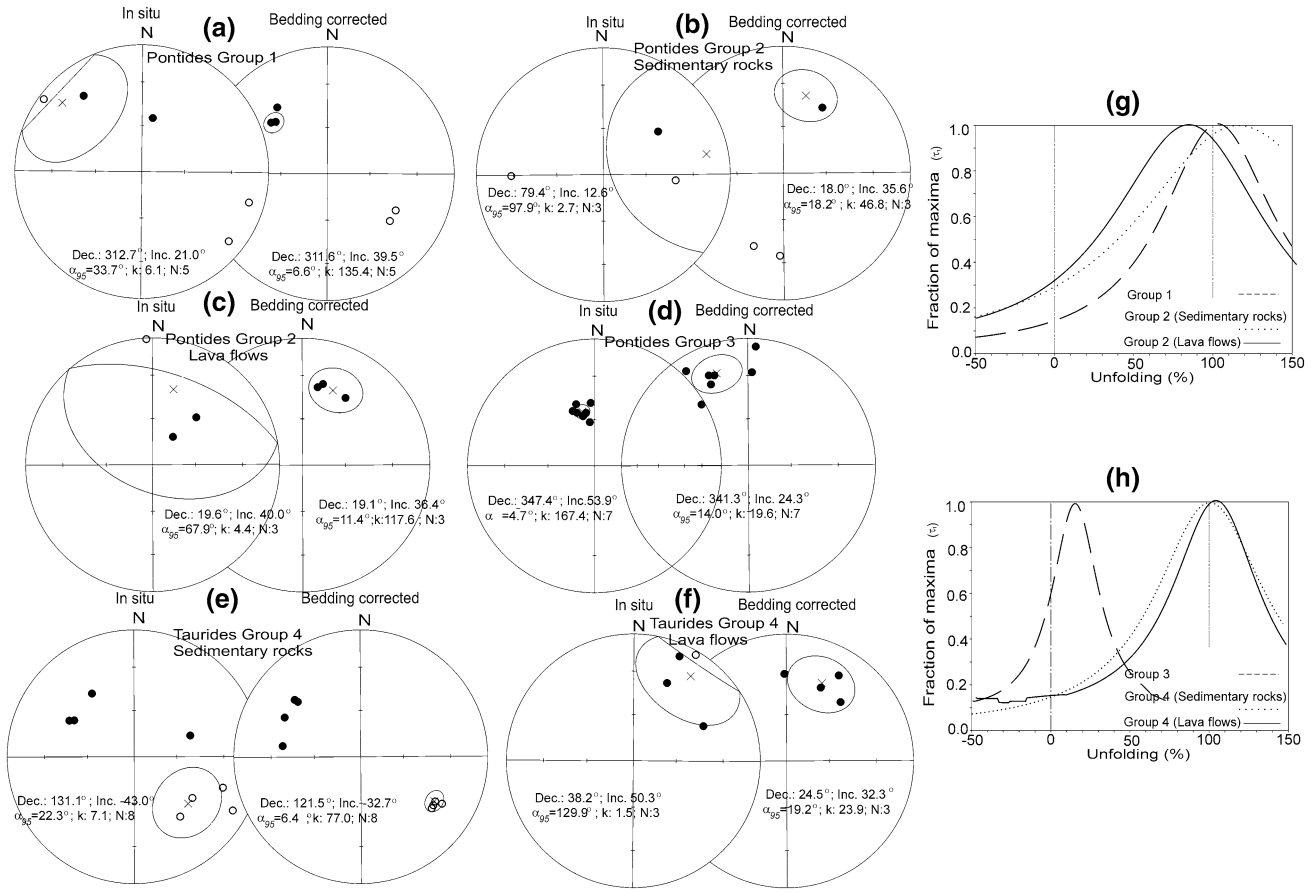

Fig. 7 Mean Paleomagnetic group mean directions from the Pontides (**a**–**d**) and the Taurides (**e**–**f**) before and after tilt correction. The Mc Fadden (1990) fold test is given for each group in 7 g and 7 h

Group 4: Elazığ-Malatya (Elazığ magmatic complex)

In the SE Taurides, the group mean direction ($N=8$) for the sedimentary rocks is $D=131.1°$, $I=-43.0°$, $\alpha_{95}=22.3°$ before, and $D=121.5°$, $I=-32.7°$ and $\alpha_{95}=6.4°$ after tilt correction (Table 1, Group 4(S), Fig. 7e). Following the statistical fold test of McElhinny (1964), the *k*-ratio ks/kg: 9.6 is higher than the critical values 2.48 at the 95% and 3.70 at the 99% level. Following the McFadden (1990) fold test, the precision parameter reaches a maximum at 98% of unfolding. The polarity test of McFadden and McElhinny (1990) shows a positive result classified with "C"at the 95% probability level (C class) with an angle between the mean directions $\gamma=4.8° < \gamma_{critic}=14.3°$.

The mean direction calculated from the sites in volcanic rocks ($N=4$) is $D=38.2°$, $I=50.3°$, $\alpha_{95}=129.9°$ before, and $D=24.5°$, $I=32.3°$ and $\alpha_{95}=19.2°$ after tilt correction (Table 1, Group 4 (L), Fig. 7f). The fold test of Mc Elhinny (1964) is negative at the 99 and 95% probability level. However, the McFadden test (1990) is positively achieved at 101% unfolding.

Paleosecular variation (PSV) should be averaged out in paleomagnetic studies so that the paleomagnetic directions present only the tectonic movement (Deenen et al. 2011). Both the lavas and the sedimentary rocks have been sampled at independent and widely spaced sites and are distributed within the geological formations over time intervals long enough to average out the geomagnetic secular variation. The criteria for paleosecular variation of the geomagnetic field developed by Deenen et al. (2011) depend on the investigation of the statistical values of paleomagnetic data sets given by the A95 cone of confidence envelopes of the VGP populations and on the number of samples (*N*). If the A95 value calculated for a mean VGP is between the lower (A_{95min}) and upper (A_{95max}) limits predicted from the geomagnetic field models, then we can conclude that the scatter observed in the VGP population is consistent with and averages of PSV. If *A*95 values are below or above the limits, then PSV should be considered unreliable (Deenen et al. 2011). In our study, the distribution of the A95 lies between A_{95min} and A_{95max} in almost all sites (Table 1), which shows that the PSV is adequately sampled in our dataset.

Discussion

Tectonic rotations

We compare the observed group mean directions with those derived from the coeval paleomagnetic pole for stable Eurasia after Torsvik et al. (2012) using R. Enkin's (unpublished data, 2004) PMGSC (version 4.2) software (Table 2).

The results show significant counterclockwise rotations with respect to stable Eurasia for most groups, while clockwise rotations with respect to Eurasia are observed within groups G2 and G4 (lavas) (Figs. 7, 8). The Upper Cretaceous arc type rocks in the Central Pontides (G1) exhibit a counterclockwise rotation of $R \pm \Delta R = -37.1° \pm 5.8°$ which is greater than the rotation estimated from Upper Cretaceous arc type rocks in Western Pontides reported in previous studies (Sarıbudak et al. 1989; Channell et al. 1996; Fig. 8). Çinku et al. (2015), reported earlier that the collision between the Pontides and the Kırşehir Block resulted in large rotations north of the Çankırı basin along the rims of the İzmir–Ankara–Erzincan Suture Zone. Indentation of the Kırşehir Block into the Central Pontides was also reported based on Middle Eocene paleomagnetic results from North Central Anatolia (Kaymakçı et al. 2003; Meijers et al. 2010; Çinku et al. 2011; Fig. 8). The significant inferred counterclockwise rotations along the NE–SW directed suture belt are similar to those observed by Çinku et al. (2015) (sites PT 21–25; Table 1; Fig. 8). When moving farher east, it can be seen that clockwise rotations of $R + \Delta R = 33.7° \pm 8.4°$ and $R + \Delta R = 29.3° \pm 6.0°$ of Group 2 is probably associated with the deformation resulting from the collision between the Kırşehir Block and the Pontides (Table 2).

Farther east in the study area, the paleomagnetic results show a secondary post-folding magnetization of the arc type rocks in Erzincan (G3), while farther north along the Eastern Pontide arc, counterclockwise rotations up to 15° have been suggested based on data obtained in previous studies (Van der Voo 1968; Channell et al. 1996; Hisarlı 2011). The deformation during Miocene time in the Erzincan basin, however, shows diverging style and magnitude of rotations, which has been interpreted to be associated with strike-slip fault motion (Tatar et al. 2013).

Large counterclockwise rotations of $R \pm \Delta R = -48.6° \pm 5.2°$ are observed in the SE Taurides for Group 4 (S). However, along a distinct line around Elazığ (including Lake Hazar), clockwise rotations of $R \pm \Delta R = +34.1° \pm 15.1°$ are observed (Table 2). The magnitude of the rotations that occured in the SE Taurides during the Late Cretaceous is partly attributed to the closure of the Southern Neotethys, which are also observed in the previous study of Cengiz Çinku et al. (2016) (Fig. 8). The contrasting sence of rotations, however, could be associated on the effect of displacement along the strands of the North and Eastern Anatolian transform faults that were active during the tectonic escape in Miocene.

Paleolatitude

Differences in declinations and similar tilt-corrected inclinations suggest that the study area experienced variable

Table 2 Group mean ChRM directions (D and I indicate declinations and inclinations after tectonic correction, respectively)

Group	Site λ, φ (N°, E°)	D_s/I_s (°)	α_{95} (°)	λ_{obs}, φ_{obs} Pole (N°, E°)	α_{95} (°)	$R \pm \Delta R$ (°)	λ(°)
G1	40.83/34.10	313.6/41.3	6.4	47.9/297.1	6.1	-37.1 ± 5.8	$23.8^{+4.2}_{-3.8}$
G2(S)	40.00/36.50	24.3/36.6	11.1	61.4/161.7	9.9	33.7 ± 8.4	$20.2^{+1.3}_{-1.2}$
G2(L)	40.00/36.50	19.9/35.7	7.5	63.5/169.5	6.6	29.3 ± 6.0	$20.4^{+1.4}_{-1.4}$
G4(S)	38.50/38.41	121.5/−32.6	6.4	35.9/304.7	5.4	-48.6 ± 5.2	$16.2^{+1.9}_{-1.8}$
G4(L)	38.50/38.41	24.5/32.3	19.2	60.6/165.1	16.6	34.1 ± 15.1	$16.8^{+4.2}_{-3.8}$

The reference pole in the Late Cretaceous (λ_{ref}, φ_{ref} = 81.3°,188.6°, α_{95} = 7.0°) is obtained after Torsvik et al. (2012). Here α_{95} is the statistical parameters after Fisher (1953). R is the angle of vertical axis rotation (positive indicates clockwise rotation) with respect to the direction computed from the stable Eurasia paleomagnetic pole with 95% confidence limit ΔR (after Demarest 1983). The paleolatitude (λ) is calculated after Enkin and Watson (1996) for inclination-only data. (*G* Group, *S* Sediments, *L* lavas). Inclination only applied for sites PT 15–17, 19, 20 in G1: geographic coordinates:$24.9^{+40.8}_{-20.3}$, $k = 6.4$; stratigraphic coordinates: 41.4 ± 5.4, $k = 87.5$ [maximum at 100% unfolding after Enkin and Watson (1996)]. Sites PT 26, 29, 32, 34 in G2(s): geographic coordinates: 39.5 ± 5.9, $k = 90.2$; stratigraphic coordinates: 36.3 ± 1.9, $k = 843.7$ [maximum at 100% unfolding after Enkin and Watson (1996)]. Sites PT 27, 28, 31, 33 in G2(v): geographic coordinates: $45.0^{+36.8}_{-29.5}$, $k = 2.3$; stratigraphic coordinates: 36.6 ± 2.1, $k = 724.9$ [maximum at 100% unfolding after Enkin and Watson (1996)]. Sites PT48, 49, 51, 57,−60, 62, 63 in G4(s): geographic coordinates:38.6 ± 7.8, $k = 23.2$; stratigraphic coordinates:30.1 ± 3.1, $k = 146.5$ [maximum at 100% unfolding after Enkin and Watson (1996)]. Sites PT52, 53, 54, 56 in G4(v): geographic coordinates:$21.9^{+39.1}_{-21.1}$, $k = 6.3$; stratigraphic coordinates:31.1 ± 6.4, $k = 77.1$ [maximum at 90% unfolding after Enkin and Watson (1996)]

amounts of vertical-axis rotations. Hence, inclination only fold test of Enkin and Watson 1996 was applied (Table 2).

The arc type rocks which were sampled in the area between the Kırşehir Block and the Central Pontides exhibit a paleolatitude of $\lambda = 23.8^{+4.2}_{-3.8}$°N (Table 2; G1). Along the trace of the İAESZ to the east, paleolatitude of $\lambda = 20.2^{+1.3}_{-1.2}$°N and $20.4^{+1.4}_{-1.4}$°N are obtained for Group 2 (Table 2; Fig. 9). This paleolatitude is obtained from the sedimentary and volcanic rocks of arc type sequences in the uppermost part of the ophiolitic suite. The results from the Eastern Pontide arc (Channell et al. 1996; Hisarlı 2011) show paleolatitudes between $\lambda = 25.\pm4.5$°N and $\lambda = 26.6^{+5.1}_{-4.6}$°N, respectively (Fig. 9) (Rice et al. 2006). The difference between the NVB and SVB succession/overlying sedimentary rocks in the Central-Eastern Pontides is approximately 5°, when considering a mean paleolatitude of ~2°N for the southern zone, and a mean paleolatitude of ~26°N for the northern zone (Fig. 10a). This could be taken alternatively as evidence of two different subduction zones during the Late Cretaceous. Alternatively, we consider the possibility that the widespreading magmatism in the Pontides during the Late Cretaceous migrated southwards after the emplacement of the volcanic arc in the Central-Eastern Pontides during the Turonian–Campanian (Çinku et al. 2010). In the Latest Cretaceous, an extensional stress-regime was active in the East Pontide arc. Thus, the southern margin of the Eastern Pontide arc extended in response to slab steepening and the volcanism moved to the South, producing the southern volcanic belt (Fig. 10b).

In the southeastern Taurides (Group 4), where the southern Neotethys suture zone has been located (Yılmaz et al. 1997a, b; Robertson et al. 2009) we have obtained data that imply paleolatitude of λ =16.2 +1.9 −1.8°N and 16.8 + 4.2 −3.8°N for the arc type sedimentary and

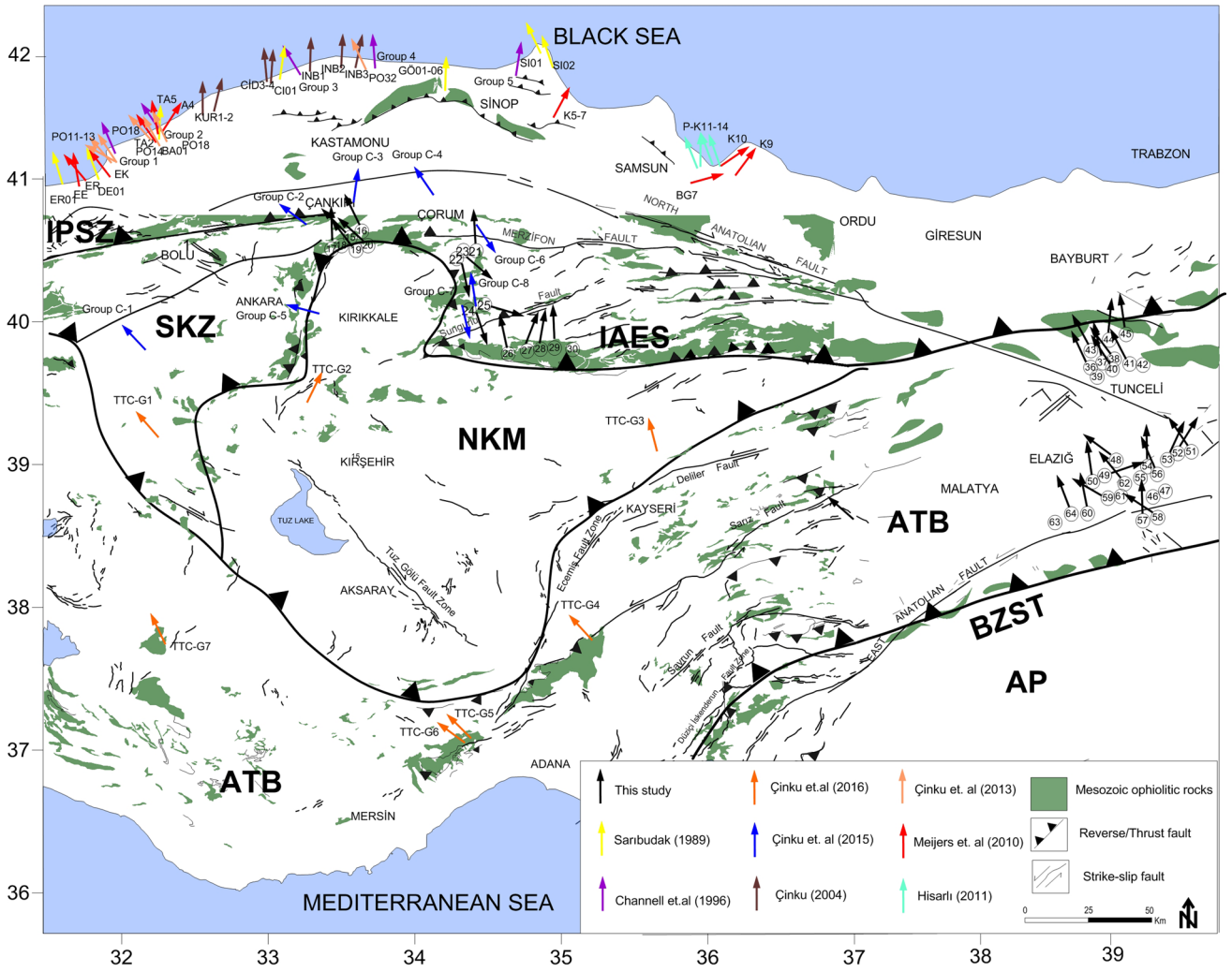

Fig. 8 Paleomagnetic declinations obtained from this and previous studies. *BZST* Bitlis Zaros Suture Zone, *IAES* Izmir Ankara Erzincan suture, *İTSZ* IntraTauride Suture Zone, *SKZ* SakaryaZ, *NKM* Niğde-Kırşehir Massif, *ATB* Anatolide-Tauride Block, *AP* Arabian Platform

volcanic rocks, respectively (Table 2; Fig. 9). A systematic decrease in Late Cretaceous paleolatitudes from the Sakarya Zone (TTC-G1), Kırşehir Block (TTC-G2,3) through the Eastern Taurides (TTC-G4,5,6) could be also seen in the study of Cengiz Çinku et al. (2016) (Fig. 9). On the Anatolide-Tauride Platform, the small difference in paleolatitude between the Pontide arc (~20°N (Table 2, G2) and the Tauride arc (Table 2, G4, ~16.5°N) suggests at this time a small basin existed in the northern branch of the Neotethys (Fig. 10a).

Comparing the paleolatitudes obtained from the Pontides and the Southeastern Taurides, a small but statistically significant difference is observed, hinting at the possibility of, two different subduction zones in the Northern Neotethys ocean. The first subduction zone in the Northern Pontides subducted earlier in the Late Cretaceous. It was suggested that the angle of subduction of the northward dipping Neotethyan slab increased considerably in Latest Cretaceous due to slab roll-back process and that the East Pontide margin extended. This extension is believed to have led to the opening of a new marginal basin from the Eastern Black Sea coast to Amasya (Beldağ basin, Yılmaz et al. 1997a, b) in the Latest Cretaceous. To the South, another subduction zone in the SE Taurides closed progressively towards the end of the Late Cretaceous until the Miocene (Cengiz Çinku et al. 2016).

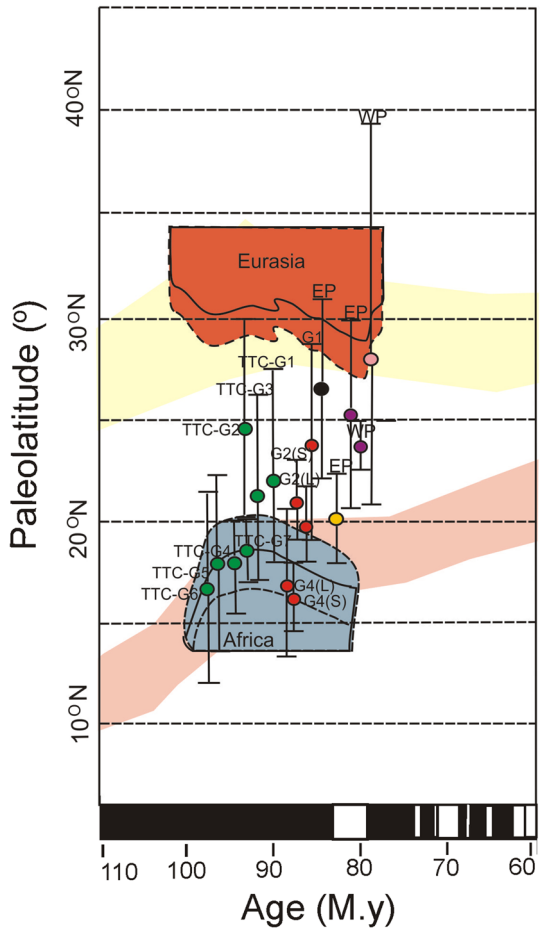

Fig. 9 Age versus reference palaeolatitude curve with error envelopes derived from the Apparent Polar Wander Path (APWP) paths of Eurasia and Gondwana for a locality near Pontides (41°N, 36°E) after Torsvik et al. (2012). Previous paleomagnetic data are taken from Channell et al. (1996) (*purple circle*), Çinku et al. (2010 (*yellow circle*), 2013 (*pink circle*), 2016 (*green circle*)), Hisarlı (2011) (*black circle*) with *error bars*. The *red circles* correspond to the results of this study. Paleomagnetic results from Cengiz Çinku et al. (2016) correspond to the Sakarya Zone (TTC-G1), Niğde-Kırşehir Massif (TTC-G2, G3), Eastern Taurides (TTC-G4,G5,G6) and Central Taurides (TTC-G7)

Conclusions

The present paleomagnetic study is associated with the following results:

a. All rocks investigated show primary magnetizations carried by pseudo-single domain magnetite or hematite, except the arc type rocks from the Karadağ lavas in Erzincan (Group 3) which exhibit a secondary post-folding remanence of the characteristic component
b. The southern magmatic belt in the Pontides deviated from a second spreading centre which points to a more than 5° southerly paleolatitude with respect to the northern spreading centre. The mechanism is interpreted to be due to a slab-roll back process of the Northern branch of the Neotethys (Rice et al. 2009; Çinku et al. 2010). An alternative would be the existence of double subduction zones in Late Cretaceous; one along the southern edge of the Pontides continental margin, generating the NVB and the other, an intra-oceanic subduction zone further S, producing the SVB.
c. The arc type rocks in the SE Taurides deviated from the Southern Neotethys ocean indicate a paleolatitude of $16.2^{+1.9}_{-1.8}$°N and $16.8^{+4.2}_{-3.8}$ in the Late Cretaceous. This implies that a small basin between the magmatic belt in the SE Taurides and the southern belt along the Pontides exist.
d. The Late Cretaceous paleomagnetic rotations in the Pontides follow a general trend in concordance with the shape of the suture zone which is formed due to the collision between the Pontides and the Kırşehir block. Farther east along the suture zone, counterclockwise rotations are influenced by both the collision phase and the westwards excursion of the Anatolian plate during the Miocene time to present. This kind of deformation is also observed in the SE Taurides, in the collision regime with the Arabian platform and the westward movement of Anatolia.

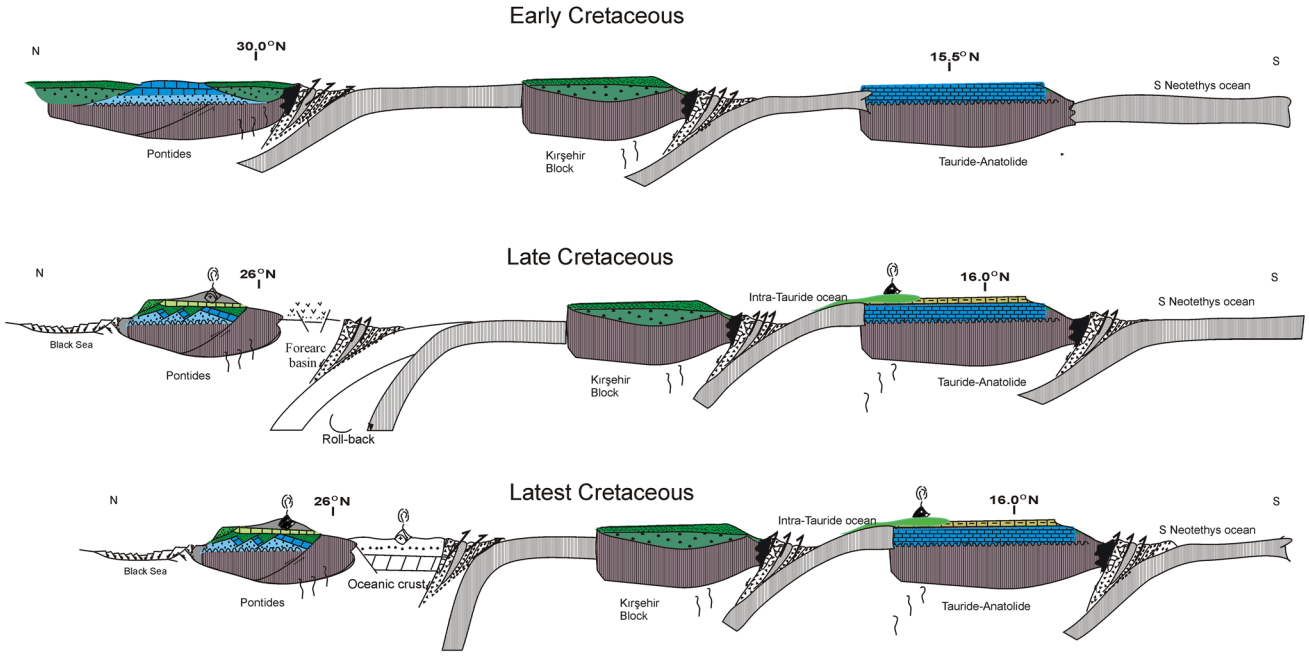

Fig. 10 The paleo(geographic) position of the Pontides and the Southeast Taurides in the Late Cretaceous

Acknowledgements This study was financially supported by the Scientific Research Projects Coordination Unit of Istanbul University (Project number 7272). We would like to thank Kenan Cinku for his help in the field work. Erwin Appel is very much appreciated for his kindly help by using the paleomagnetic laboratory in the University of Tübingen. Nurcan Kaya is thanked for her help in paleomagnetic measurements. Prof. Dr. John Geissman and one anonymous reviewer are very much appreciated for their helpful suggestions.

References

Aktaş G, Robertson HF (1984) The Maden Complex, S E Turkey : evolution of a Neotethyan active margin In: Dixon JE, Robertson AHF (eds) The geological evolution of the Eastern Mediterranean. Published for The Geological Society by Blackwell Scientific Publication Oxford London Edinburgh Boston Palo Alto Melbourne, New Jersey pp 375–401

Aygül M, Okay AI, Oberhansli R, Schmidt A, Sudo, Masafumi (2015) Late Cretaceous infant intra-oceanic arc volcanism, the Central Pontides, Turkey: petrogenetic and tectonic implications. J Asian Earth Sci. doi:10.1016/j.jseaes.2015.07.005

Beyarslan M, Bingöl AF (2000) Petrology of a supra-subduction zone ophiolite (Elazığ Turkey). Can J Earth Sci 37:1411–1424

Birgili S, Yoldaş R, Nalan UG (1974) The geology of Cankırı-Corum basin and a preliminary report on its petroleum possibilities. TPC Report No: 1216 (unpublished)

Boulton SJ (2009) Record of Cenozoic sedimentation from the Amanos Mountains, Southern Turkey: implications for the inception and evolution of the Arabia-Eurasia continental collision. Sediment Geol 216:29–47

Boulton SJ, Robertson AHF, Unlügenç ÜC (2006) Tectonic and sedimentary evolution of the Cenozoic Hatay Graben, Southern Turkey: a two-phase, foreland basin then transtensional basin model. In: Robertson AHF, Mountrakis D (eds) Tectonic Evolution of the Eastern Mediterranean. Geological Society (Special Publications) 260, pp 613–634

Bozkurt E, Winchester JA, Yiğitbaş E, Ottley CJ (2008) Proterozoic ophiolites and maficultramafic complexes marginal to the İstanbul Block: an exotic terrane of Avalonian affinity in NW Turkey. Tectonophysics 461:240–251. doi:10.1016/j.tecto.2008.04.027

Boztuğ D (2000) S–I–A-type intrusive associations: geodynamic significance of synchronism between metamorphism and magmatism in Central Anatolia, Turkey. In: Bozkurt E, Winchester J, Piper JA (eds) Tectonics and Magmatism in Turkey and the Surrounding Area. Geol Soc Lond Spec Publ 173:407–424

Boztuğ D, Jonckheere RC (2007) Apatite fission-track data from central-Anatolian granitoids (Turkey): constraints on Neo-Tethyan closure. Tectonics 26:TC3011

Boztuğ D, Arehart GB, Platevoet B, Harlavan Y, Bonin B (2007) High-K calc-alkaline I-type granitoids from the composite Yozgat batholith generated in a postcollisional setting following continent-oceanic island arc collision in central Anatolia, Turkey. Mineral Petrol 91:191–223

Cengiz Çinku M, Hisarli ZM, Yılmaz Y, Ülker B, Kaya N, Öksüm E et al (2016) The tectonic history of the Niğde-Kırşehir Massif and the Taurides since the Late Mesozoic: Paleomagnetic evidence for two-phase orogenic curvature in Central Anatolia, Tectonics 35:772–811

Channell JET, Tüysüz O, Bektaş¸ O, Şengör, AM (1996) Jurassic-Cretaceous paleomagnetism and paleogeography of the Pontides (Turkey). Tectonics 15(1):201–212

Çinku MC (2011) Paleogeographic evidence on the Jurassic tectonic history of the Pontides: new paleomagnetic data from the Sakarya continent and Eastern Pontides. Int J Earth Sci 100(7):1633–1645

Çinku MC, Hirt AM, Hisarlı ZM, Heller F, Orbay N (2010) Southward migration of arc magmatism during latest Cretaceous associated with slab steepening, East Pontides, N Turkey: new paleomagnetic data from the Amasya region. Phys Earth Planet Inter 182:18–29

Çinku MC, Hisarlı MZ, Heller F, Orbay N, Ustaömer T (2011) Middle Eocene paleomagnetic data from the eastern Sakarya zone and the central pontides: implications for the tectonic evolution of north central Anatolia. Tectonics 30:TC1008

Çinku MC, Hisarlı MZ, Hirt AM, Heller F, Ustaömer T, Kaya N, Öksüm E, Orbay N (2015) Evidence of late cretaceous oroclinal bending in north-central anatolia: paleomagnetic results from Mesozoic and Cenozoic rocks along the Izmir-Ankara-Erzincan Suture Zone. Geological Society Special Issue; Palaeomagnetism in Fold and Thrust Belts: New Perspectives; Edt. Belen Oliva Urcia Geol. Soc. London Spec. Publ., 08/2015; doi:10.1144/SP425.2

Day R, Fuller MD, Schmidt VA (1977) Hysteresis Properties of Titanomagnetites: Grain Size And Composition Dependence. Phys Earth Planet Int 13:260–267

Deenen MHL, Langereis CG, van Hinsbergen DJJ, Biggin AJ (2011) Geomagnetic secular variation and the statistics of palaeomagnetic directions. J Geophys Int 186:509–520

Demarest HH Jr (1983) Error analysis for the determination of tectonic rotation from paleomagnetic data. J Geophys Res 88:4321–4328, doi:10.1029/JB088iB05p04321

Dunlop DJ (2002) Theory and application of the Day plot (Mrs/Ms versus Hcr/Hc) 2. Application to data for rocks, sediments, and soils. J Geophys Res 107(B3). doi:10.1029/2001JB000487

Dunlop DJ, Özdemir Ö (1997) Rock Magnetism: Fundamentals and Frontiers. Vol 573, Cambridge University Press, New York

Enkin RJ, Watson GS (1996) Statistical analysis of paleomagnetic inclination data. J Geophys Int 126:495–504

Erdoğan B, Akay E, Şirin Uğur M (1996) Geology of the Yozgat region and evolution of the collisional Çankırı Basin. Inter Geol Rev 38:788–806

Fisher RA (1953) Dispersion on a sphere. Proc R Soc Lond 217:195–305

Floyd PA, Yalınız MK, Göncüoğlu MC (1998) Geochemistry and petrogenesis of intrusive and extrusive ophiolitic plagiogranites, central Anatolian Crystalline Complex, Turkey. Lithos 42:225–241

Gans CR, Beck SL, Zandt G, Berk CB, Ozacar AA (2009) Detecting the limit of the slab break-off in Central Turkey: new high-resolution Pn tomography results. Geophys J Int 179:1566–1572

Göncüoğlu MC, Toprak V, Kuscu I, Erler A, Olgun E (1991) Geology of the western part of the Central Anatolian Massif, Part 1: Southern Section: Unpubl. Report No.2909, Turkish Petroleum Company Report (in Turkish)

Görür N, Tüysüz O (1997) Petroleum geology of the southern continental margin of the Black Sea. In: Robinson AG (ed), Regional and Petroleum Geology of the Black Sea and Surrounding Region, AAPG Memoir, vol. 68. AAPG, Tulsa, OK, pp 241–254

Hisarlı ZM (2011) New paleomagnetic constraints on the late Cretaceous and early Cenozoic tectonic history of the Eastern Pontides. J Geodyn 52:114–128

İlbeyli N, Pearce JA, Thirwall MF, Mitchell JG (2004) Petrogenesis of collision related plutonics in central Anatolia, Turkey. Lithos 72:163–182

Jelínek V (1977) The statistical theory of measuring anisotropy of magnetic susceptibility of rocks and its applications. Geofyzika Brno 88

Kadıoğlu YK, Dilek Y, Foland KA (2006) Slab breakoff and syncollisional origin of the Late Cretaceous magmatism in the Central Anatolian Crystalline Complex, Turkey. In: Dilek Y, Pavlides S (eds) Postcollisional Tectonics and Magmatism in the Mediterranean Region and Asia. Geol. Soc. America, Boulder, CO, Special Papers, 409:381–415

Karaoğlan F, Parlak O, Klötzli U, Thöni M, Koller F (2013) U-Pb and Sm-Nd geochronology of the Kızıldağ (Hatay, Turkey) ophiolite: implications for the timing and duration of suprasubduction zone type oceanic crust formation in southern Neotethys. Geol Mag 150:283–299

Karıg DE, Kozlu H (1990) Late Palaeogene evolution of the triple junction region near Maraş south-central Turkey. J Geol Soc London 147:1023–1034

Kaymakçı N, Duermeijer CE, Langereis C, White SH, VAN DIJK PM (2003) Palaeomagnetic evolution of the Cankırı Basin (central Anatolia, Turkey): implications for oroclinal bending due to indentation. Geological Magazine 140:343–355

Kaymakçı N, Özçelik Y, White SH, van Dijk PM (2009) Tectono-stratigraphy of the Çankırı Basin: Late Cretaceous to early Miocene evolution of the Neotethyan Suture Zone in Turkey. In: van Hinsbergen DJ, Edwards MA, Govers R (eds) Collision and Collapse at the Africa–Arabia–Eurasia Subduction Zone, Geol Soc Lond Spec. Publ. 311:67–106

Kirschvink JL (1980) The least-squares line and plane and the analysis of palaeomagnetic data. Geophy J R Astron Soc 62:699–718

Kozlu H (1997) Tectono-stratigraphic units of the Neogene basins (Iskenderun, Misis Andırın) and their tectonic evolution in the eastern Mediterranean region. Unpublished PhD Thesis. Çukurova University, Natural Science Institute, Adana-Turkey (Turkish)

Kröner A, Şengör AMC (1990) Archean and Proterozoic ancestry in late Precambrian to early Paleozoic crustal elements of southern Turkey as revealed by single-zircon dating. Geology 18:1186–1190

Lefebvre C, Meijers MJM, Kaymakçı N, Peynircioğlu A, Langereis CG, van Hinsbergen DJJ (2013) Reconstructing the geometry of central Anatolia during the Late Cretaceous: large-scale Cenozoic rotations and deformation between the Pontides and Taurides. EPSL 366:83–98. doi:10.1016/j.epsl.2013.01.003

Lowrie W (1990) Identification of ferromagnetic minerals in a rock by coercivity and unblocking temperature properties. Geophys Res Lett 17:159–162

McElhinny MW (1964) Statistical significance of the fold test in palaeomagnetism. Geophys J R Astron Soc 8:338–340. doi:10.1111/j.1365-246X.1964.tb06300.x

McFadden PL (1990) The fold test as an analytical tool. Geophy J Inst 135:329–338

McFadden PL, McElhinny MW (1990) Classification of the reversal test in palaeomagnetism. Geophy J Int 103:725–729

Meijers MJM, Kaymakçı N, Van Hinsbergen DJJ, Langereis CG, Stephenson RA, Hippolyte J-C (2010) Late Cretaceous to Paleocene oroclinal bending in the Central Pontides (Turkey). Tectonics 29:TC4016. doi:10.1029/2009TC002620

Michard A, Whitechurch H, Rico LE, Montigny R, Yazgan E (1984) Tauric subduction (Malatya-Elazığ provinces) and its bearing on tectonics of the Tethyan realm in Turkey. In: Dixon JE, Robertson AHF (eds) The Geological Evolution of the Eastern Mediterranean. Blackwell Scientific Publications, Oxford, pp 361–373

MTA (2002) Geological Map of Turkey, 1:500,000, Maden Tektik ve Arama Genel Müdürlüğü (General Directorate of Mineral Research and Exploration), Ankara

Nairn S (2011) Testing alternative models of continental collision in Central Turkey by a study of the sedimentology, provenance and tectonic setting of Late Cretaceous–Early Cenozoic syn-tectonic sedimentary basins. PhD thesis, Edinburgh University, p 395

Nairn SP, Robertson AHF, Ünlügenç UC, Taslı K, Inan N (2012) Tectonostratigraphic evolution of the Upper Cretaceous-Cenozoic central Anatolian basins: an integrated study of diachronous ocean basin closure and continental collision. In: Robertson AHF, Parlak O, Ünlügenç UC (eds) Geological Development of Anatolia and the Easternmost Mediterranean Region. Geol. Soc. Lond. Spec. Publ. 372:343–384. doi:10.1144/SP372.9

Okay AI, Şahintürk O (1997) Geology of the Eastern Pontides. In: Robinson AG (ed) Regional and Petroleum Geology of the Black

Sea and Surrounding Region. American Association Petroleum Geology Memoirs 68, 291–311.
Okay AI, Tüysüz O (1999) Tethyan Sutures of Northern Turkey. In: Durand B, Jolivet L, Hovarth F, Séranne M (eds) The Mediterranean Basins, Tertiary Extension within the Alpine Orogen. Geol. Soc. Lond. Spec. Publ. 156:475–515
Okay AI, Satir M, Maluski H, Siyako M, Monie P, Metzger R, Akyüz S (1996) Paleo- and Neo-Tethyan events in northwestern Turkey: Geologic and geochronologic constraints. In: Yin A, Harrison TM (eds) The tectonic evolution of Asia. Cambridge, UK and New York, Cambridge University Press, Cambridge pp 420–441
Okay AI, Satır M, Shang CK (2008) Ordovician metagranitoid from the Anatolide-Tauride Block, northwest Turkey–geodynamic implications. Terra Nova 20:280–288
Okay AI, Zattin M, Cavazza W (2010) Apatite fissiontrack data for the Miocene Arabia-Eurasia collision. Geology 38:35–38. doi:10.1130/G30234.1
Okay AI, Sunal G, Sherlock S, Altiner D, Tüysüz O, Kylander-Clark ARC, Aygül M (2013) Early Cretaceous sedimentation and orogeny on the southern active margin of Eurasia: Central Pontides. Tectonics 32:1247–1271. doi:10.1002/tect.20077
Okay AI, Altıner D, Kılıç AM (2015) Triassic limestone, turbidite and serpentinite – Cimmeride orogeny in the Central Pontides: Geological Magazine. doi:10.1017/S0016756814000429
Özcan A, Erkan A, Keskin A, Oral A, Özer S, Sümengen M, Tekel O (1980) Geology of the Area Between the North Anatolian Fault and the Kırşehir Massif. Maden Tetkik ve Arama Enstitüsü (MTA) Report No. 6722 (in Turkish, unpublished)
Özgül N, Turşucu A (1984) Stratigraphy of the Mesozoic Carbonate Sequence of the Munzur Mountains (Eastern Taurides). In: Tekeli O, Göncüoğlu MC (eds) Geology of the Taurus Belt, Ankara, 173–181
Parlak O, Rızaoğlu T, Bağcı U, Karaoğlan F, Höck V (2009) Tectonic significance of the geochemistry and petrology of ophiolites in southeast Anatolia, Turkey. Tectonophysics 473:173–187
Perinçek D (1979) The Geology of Hazro–Korudağ–Çüngüsc–Maden–Ergani–Hazar–Elazığ –Malatya Area. Special Publication of the Geological Society of Turkey, Ankara
Rice SP, Robertson AHF, Ustaömer T (2006) Late Cretaceous-Early Cenozoic tectonic evolution of the Eurasian active margin in the central and eastern Pontides, northern Turkey. In: Robertson AHF, Mountrakis D (eds) Tectonic development of the eastern Mediterranean region. Geol. Soc. Lond. Spec. Publ., vol 260 pp 413–445
Rice SP, Roberson, A.H.F., Ustaömer T, İnan T, Taslı K (2009) Late Cretaceous-Early Eocene tectonic development of the Tethyan Suture Zone in the Erzincan area, eastern Pontides, Turkey. Geol Mag 146(4):567–590
Rızaoğlu T, Parlak O, Höck V, Koller F, Hames WE, Billor Z (2009) Andean-type active margin formation in the eastern Taurides: geochemical and geochronogical evidence from the Baskil granitoid (Elazığ, SE Turkey). Tectonophysics 473:188–207
Robertson AHF (2006) Contrasting modes of ophiolite emplacement in the Eastern Mediterranean region. In: GEE D, Stephenson RA (eds) European Lithosphere Dynamics. Geol. Soc. London, Memoir 32:235–261
Robertson AHF, Dixon JD (1984) Introduction: aspects of the geological evolution of the eastern Mediterranean. In: Dixon JE, Robertson AHF (eds) The geological evolution of the eastern Mediterranean. Geol. Soc. Lond. Spec. Publ., 17:1–74
Robertson AH, Ustaömer T, Pickett EA, Collins AS, Andrew T, Dixon JE (2004) Testing models of Late Palaeozoic-Early mesozoic orogeny in western Turkey: support for an evolving open-tethys model. J Geol Soc 161:501–511
Robertson A, Ustaömer T, Parlak O, Ünlügenç UC, Taslı K, İnan N (2006) The Berit transect of the Tauride thrust belt, S. Turkey: late Cretaceous-Early Cenozoic accretionary/collisional processes related to closure of the southern Neotethys. J Asian Earth Sci 27:108–145
Robertson AHF, Parlak O, Rızaoğlu T, Ünlügenc¸ U, İnan N, Taşlı K, Ustaömer T (2007a) Tectonic evolution of the South Tethyan Ocean: evidence from the Eastern Taurus Mountains (Elazığ region, SE Turkey). In: Ries AC, Butler RWH, Graham RH (eds) Deformation of the continental crust: the legacy of mike coward. Geol. Soc. Lond. Spec. Publ. vol 272, 231–270
Robertson A, Ustaomer T, Parlak O, Unlugenc UC, Tasli K, Inan N (2007b) The Berit transect of the Tauride thrust belt, S Turkey: Late Cretaceous-Early Cenozoic accretionary/collisional processes related to closure of the Southern Neotethys (vol 27, pg 108, 2006) J Asian Earth Sci 29(5–6):978–980 **(3 p)**
Robertson AH, Parlak O, Ustaömer T, 2009. Melange Genesis And Ophiolite Emplacement Related To Subduction Of The Northern Margin Of The Tauride-Anatolide Continent, Central And Western Turkey. In: van Hinsbergen DJJ, Edwards MA, Govers R (eds) Collision and Collapse at the Africa-Arabia-Eurasia Subduction Zone. Geol. Soc. London, pp 9–66
Robertson AH, Parlak O, Ustaömer T (2013) Late Palaeozoic Early Cenozoic tectonic development of Southern Turkey and the easternmost Mediterranean region: evidence from the interrelations of continental and oceanic units. Geological Society, London, Special Publications 2013, vol 372, pp 9–48
Robertson AHF, Parlak O, Ustaömer T, Taşlı K, İnan N, Dumitrica P, Karaoğlan F (2014) Subduction, ophiolite genesis and collision history of Tethys adjacent to the Eurasian continental margin: New evidence from the Eastern Pontides, Turkey. Geodin Acta. 10.1080/09853111.2013.877240
Sarıbudak M (1989) New results and a palaeomagnetic overview of the Pontides in Northern Turkey. Geophys. J Int 99:521–531
Şengör AMC (1979) The North Anatolian fault: Its age, offset, and tectonic significance. J Geol Soc Lond 136:268–282
Şengör AMC (1984) The Cimmeride orogenic system and the tectonics of Eurasia, Geol. Soc. America Spec. Paper 195:82
Şengör AMC, Yılmaz Y (1981) Tethyan evolution of Turkey: a plate tectonic approach. Tectonophysics 75:181–241
Stampfli GM (2000) Tethyan oceans. In: Bozkurt E, Winchester JA, Piper JDA (eds) Tectonics and Magmatism in Turkey and the Surrounding Area. Geol. Soc. Lond. Spec. Publ. vol 173, pp 1–23
Tatar O, Akpinar Z, Gürsoy H, Piper, J.D.A., Koçbulut F, Mesci BL, Polat A, Roberts AP (2013) Palaeomagnetic evidence for the neotectonic evolution of the Erzincan Basin, North Anatolian Fault Zone, Turkey. J Geodynamics 65:244–258
Tekeli O (1981) Subduction complex of pre-Jurassic age, northern Anatolia, Turkey. Geology 9:68–72
Torsvik TH, Van der Voo R, Preeden U, Mac Niocaill C, Steinberger B, Doubrovine PV, van Hinsbergen DJJ, Domeier M, Gaina C, Tohver E, Meert JG, McCausland PJA, Cocks LRM (2012) Phanerozoic polar wander, palaeogeography and dynamics. Earth Sci Rev 114(3–4):325–368
Tüysüz O (1990) Tectonic evolution of a part of the Tethyside orogenic collage: the Kargı Massif, northern Turkey. Tectonics 9:141–160
Tüysüz O (1999) Geology of the Cretaceous sedimentary basins of the western Pontides. Geol J 34:75–93. doi:10.1002/(SICI)1099-1034(199901/06)34:1/23.0.CO;2-S
Tüysüz O, Dellaloğlu, AA, Terzioğlu N (1995) A magmatic belt within the Neo-Tethyan suture zone and its role in the tectonic evolution of northern Turkey. Tectonophysics 243:173–191
Tüysüz O, Yılmaz İÖ, Svabenicka L, Kırıcı S (2012) The Unaz formation: a key unit in the Western Black Sea region, N Turkey. Turk J Earth Sci 21:1009e1028. doi:10.3906/yer-1006-30

Ustaömer T, Robertson AHF (1993) A Late Palaeozoic–Early Mesozoic marginal basin along the active southern continental margin of Eurasia: evidence from the Central Pontides (Turkey) and adjacent regions. Geol J 28:219–238

Ustaömer T, Robertson AH (1994) Late Palaeozoic Marginal Basin And Subduction-Accretion: the Palaeotethyan Küre Complex, Central Pontides, Northern Turkey. J Geol Soc 151:291–305

Ustaömer T, Robertson AHF (1997) Tectonic–sedimentary evolution of the North-Tethyan active margin in the central Pontides of Northern Turkey. In: Robinson AG (ed.) Regional and petroleum geology of the Black Sea region, vol 68. AAPG Memoir, pp 245–290

Van der Voo R (1968) Jurassic, Cretaceous end Eocene pole position from northeastern Turkey. Tectonophysics 6(3):251–269

Yalınız MK, Göncüoğlu MC, Özkan-Altıner S (2000) Formation and Emplacement Ages of the SSZ-type Neotethyan Ophiolites in Central Anatolia, Turkey: Paleotectonic Implications. Geol J 35:53–68

Yazgan E, Chessex R (1991) Geology and tectonic evolution of the southeastern Taurides in the region of Malatya. Bull Assoc Turk Pet Geol 3(1):1–42

Yiğitbas E, Elmas A, Yılmaz Y (1999) Pre-Cenozoic tectonostratigraphic components of the western Pontides and their geological evolution. Geol J 34:55–74

Yiğitbaş E, Yılmaz Y (1996) New evidence and solution to the Maden complex controversy of the Southeast Anatolian orogenic belt (Turkey). Geologische Rundschau 85(2):250–263

Yılmaz Y (1993) New evidence and model on the evolution of the southeast Anatolian orogen. Geol Soc Am Bull 105:251–271

Yılmaz Y, Yiğitbaş E, Genç ŞC (1993) Ophiolitic and metamorphic assemblages of southeast Anatolia and their significance in the geological evolution of the orogenic belt. Publ. I. T. U. Mining Faculty, 12:1280–1297

Yılmaz Y, Tüysüz O, Yiğitbas E, Genç SC, Sengör AMC (1997a) Geology and tectonic evolution of the Pontides. In: Robinson A (ed) Regional and petroleum geology of the Black Sea and surrounding region: American Association of Petroleum Geologists Memoir, no. 68, pp 183–226

Yılmaz Y, Serdar HS, Genc C, Yiğitbaş E, Gürer ÖF, Elmas A, Yıldırım M, Bozcu M, Gürpınar O (1997b) The geology and evolution of the Tokat massif, South-Central Pontides, Turkey. Int Geol Rev 39:365–382

Yoldaş¸ R (1982) The geology between Tosya (Kastamonu) and Bayat (Corum) area. PhD thesis, University of Istanbul, College of Science, 311p., (unpublished)

Zijderveld JDA (1967) AC Demagnetization of rocks: analysis of results. In: Runcorn SK, Creer KM, Collinson DW (eds) Methods in paleomagnetism pp 254–286